We are IntechOpen, the world's leading publisher of Open Access books Built by scientists, for scientists

4,800
Open access books available

122,000
International authors and editors

135M
Downloads

Our authors are among the

154
Countries delivered to

TOP 1%
most cited scientists

12.2%
Contributors from top 500 universities

CLARIVATE ANALYTICS BOOK CITATION INDEX INDEXED

WEB OF SCIENCE™

Selection of our books indexed in the Book Citation Index in Web of Science™ Core Collection (BKCI)

Interested in publishing with us?
Contact book.department@intechopen.com

Numbers displayed above are based on latest data collected.
For more information visit www.intechopen.com

14

A Plane Vibration Model for Natural Vibration Analysis of Soft Mounted Electrical Machines

Ulrich Werner
Siemens AG, Industry Drive Technologies, Large Drives, Products Development
Germany

1. Introduction

Large electrical machines, which operate at high speeds, are often designed with flexible shafts and sleeve bearings, because of the high circumferential speed of the shaft journals. Especially for industrial applications, the foundations of this kind of machines are often designed as soft foundations (Fig. 1), because of plant specific requirements. Therefore often a significant influence of the soft foundation on the vibrations exists (Gasch et al., 1984; Bonello & Brennan, 2001). Additionally to the mechanical parameters – such as e.g. mass, mechanical stiffness and damping – an electromagnetic field in the electrical machine exists, which causes an electromagnetic coupling between rotor and stator and also influences the natural vibrations (Schuisky, 1972; Belmans et al., 1987; Seinsch, 1992; Arkkio et al., 2000; Holopainen, 2004; Werner, 2006). The aim of the chapter is to show a plane vibration model for natural vibration analysis, of soft mounted electrical machines, with flexible shafts and sleeve bearings, especially considering the influence of a soft foundation and the electromagnetic field. Based on a simplified plane vibration model, the mathematical correlations between the rotor and the stator movement, the sleeve bearings, the electromagnetic field and the foundation, are shown. For visualization, the natural vibrations of a soft mounted 2-pole induction motor (rated power: 2 MW) are analyzed exemplary, especially focusing on the influence of the foundation, the oil film stiffness and damping and of the electromagnetic field.

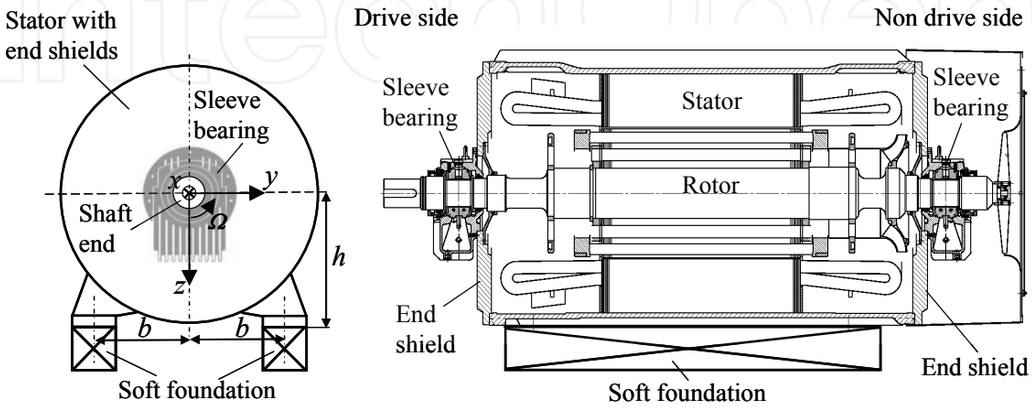

Fig. 1. Induction motor (2-pole), mounted on a soft foundation

2. Vibration model

The vibration model is a simplified plane model (Fig. 2), describing the natural vibrations in the transversal plane (plane y, z) of a soft mounted electrical machine. Therefore no natural vibrations regarding the translation in the x-axis, the rotation at the y-axis and the rotation at the z-axis are considered. The plane model is based on the general models in (Werner, 2008; Werner, 2010), but especially focusing here on the natural vibration analysis.

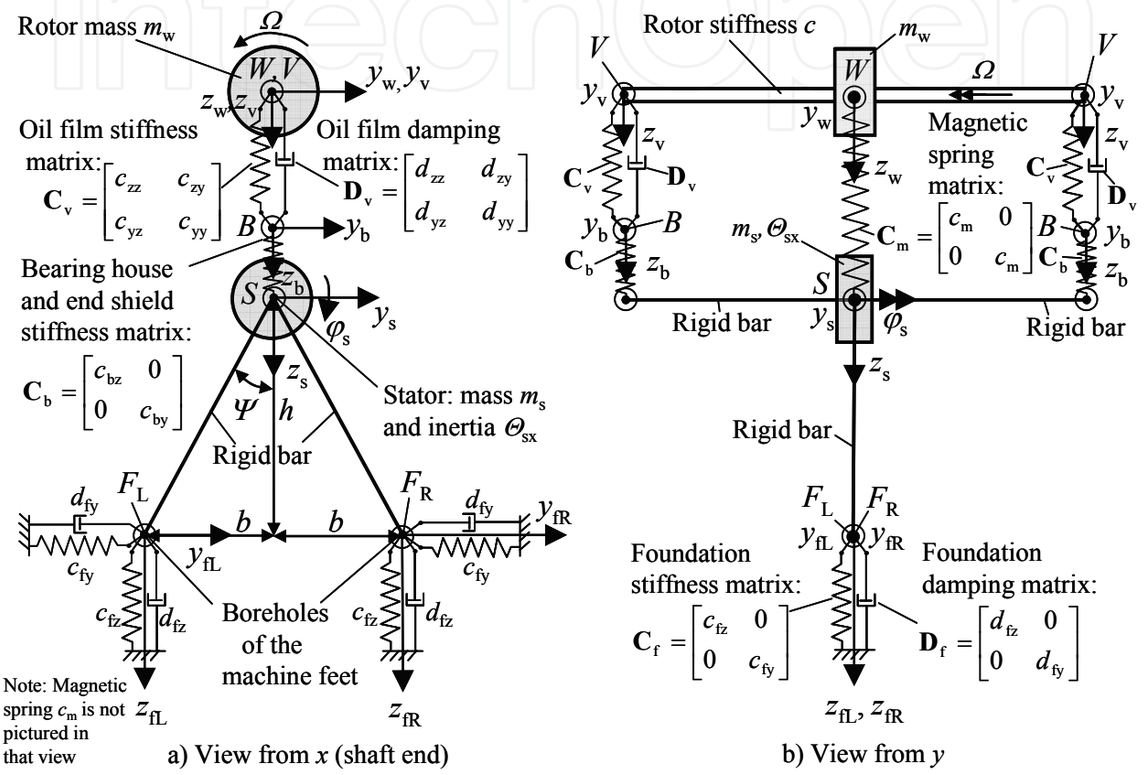

Fig. 2. Vibration model of a soft mounted electrical machine

The model consists of two masses, rotor mass m_w, concentrated at the shaft – rotating with angular frequency Ω – and stator mass m_s, which has the inertia θ_{sx} and is concentrated at the centre of gravity S. The moments of inertia of the rotor are not considered and therefore no gyroscopic effects. Shaft journal centre point V describes the movement of the shaft journal in the sleeve bearing. Point B is positioned at the axial centre of the sleeve bearing shell and describes the movement of the bearing housing. The rotor mass is mechanically linked to the stator mass by the stiffness of rotor c and the oil film stiffness matrix $\mathbf{C}_v$ and the oil film damping matrix $\mathbf{D}_v$ of the sleeve bearings, which contain the oil film stiffness coefficients (c_{yy}, c_{yz}, c_{zy}, c_{zz}) and the oil film damping coefficients (d_{yy}, d_{yz}, d_{zy}, d_{zz}) (Fig. 3). The cross-coupling coefficients – stiffness cross-coupling coefficients c_{yz}, c_{zy} and damping cross-coupling coefficients d_{yz}, d_{zy} – cause a coupling between vertical and horizontal movement and the vertical oil film force F_z and the horizontal oil film forces F_y (Tondl, 1965; Glienicke, 1966; Lund & Thomsen, 1978; Lund & Thomsen, 1987; Gasch et al. 2002; Vance et al., 2010), which is mathematically described in (1).

$$\begin{bmatrix} F_z \\ F_y \end{bmatrix} = \begin{bmatrix} c_{zz} & c_{zy} \\ c_{yz} & c_{yy} \end{bmatrix} \cdot \begin{bmatrix} z_v - z_b \\ y_v - y_b \end{bmatrix} + \begin{bmatrix} d_{zz} & d_{zy} \\ d_{yz} & d_{yy} \end{bmatrix} \cdot \begin{bmatrix} \dot{z}_v - \dot{z}_b \\ \dot{y}_v - \dot{y}_b \end{bmatrix} \tag{1}$$

For cylindrical shell bearings the cross-coupling stiffness coefficients are usually not equal ($c_{zy} \neq c_{yz}$). This leads to an asymmetric oil film stiffness matrix C_v, which is the reason that vibration instability may occur (Tondl, 1965; Glienicke, 1966; Lund & Thomsen, 1978; Lund & Thomsen, 1987; Gasch et al. 2002; Vance et al., 2010). In this model it is assumed that the drive side and the non drive side values are the same, and the bearing housing and end shield stiffness matrix C_b is also assumed to be same for the drive side and non drive side. The stiffness and damping values of the oil film are calculated by solving the Reynolds-differential equation, using the radial bearing forces, which are caused by the rotor weight and static magnetic pull. The stiffness and damping values of the oil film are assumed to be linear regarding the displacements of the shaft journals relative to the bearing housings.

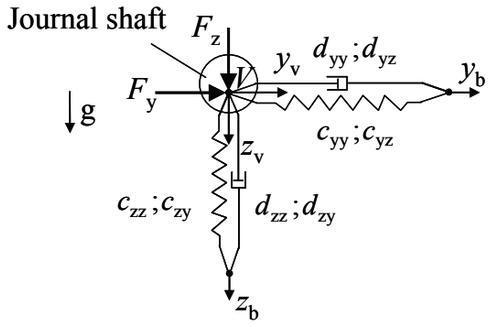

Fig. 3. Oil film forces

Damping of the bearing housings and the end shields are not considered because of the usually low damping ratio. For electrical machines, an additional magnetic stiffness matrix C_m between the rotor and the stator exists, which describes the electromagnetic coupling between the rotor and stator. The magnetic spring constant c_m has a negative reaction. This means that a radial movement between the rotor and stator creates an electromagnetic force that tries to magnetize the movement (Schuisky, 1972; Belmans et al., 1987; Seinsch, 1992; Arkkio et al., 2000; Holopainen, 2004; Werner, 2006). Here the magnetic spring coefficient c_m is defined to be positive, which acts in the direction of the magnetic forces. Electromagnetic field damping effects, e.g. by the rotor cage of an induction motor, are not considered in this paper. The stator structure is assumed to be rigid when compared to the soft foundation. The foundation stiffness matrix C_f and the foundation damping matrix D_f connect the stator feet, F_L (left side) and F_R (right side), to the ground. The foundation stiffness and damping on the right side is assumed to be the same as on the left side. The stiffness values c_{fy} and c_{fz} and the damping values d_{fy} and d_{fz} are the values for each machine side. The coordinate systems for V (z_v; y_v) and B (z_b; y_b) have the same point of origin, as well as the coordinate systems for the stator mass m_s (z_s; y_s) and for the rotor mass m_w (z_w; y_w). They are only shown with an offset to show the connections through the various spring and damping elements.

3. Natural vibrations

To calculate the natural vibrations, it is necessary to derive the homogenous differential equation, which is assumed to be linear.

3.1 Derivation of the homogenous differential equation system

The homogenous differential equation system can be derived by separating the vibration system into four single systems – (a) rotor mass system, (b) journal system, (c) bearing house system and (d) stator mass system – (Fig. 4).

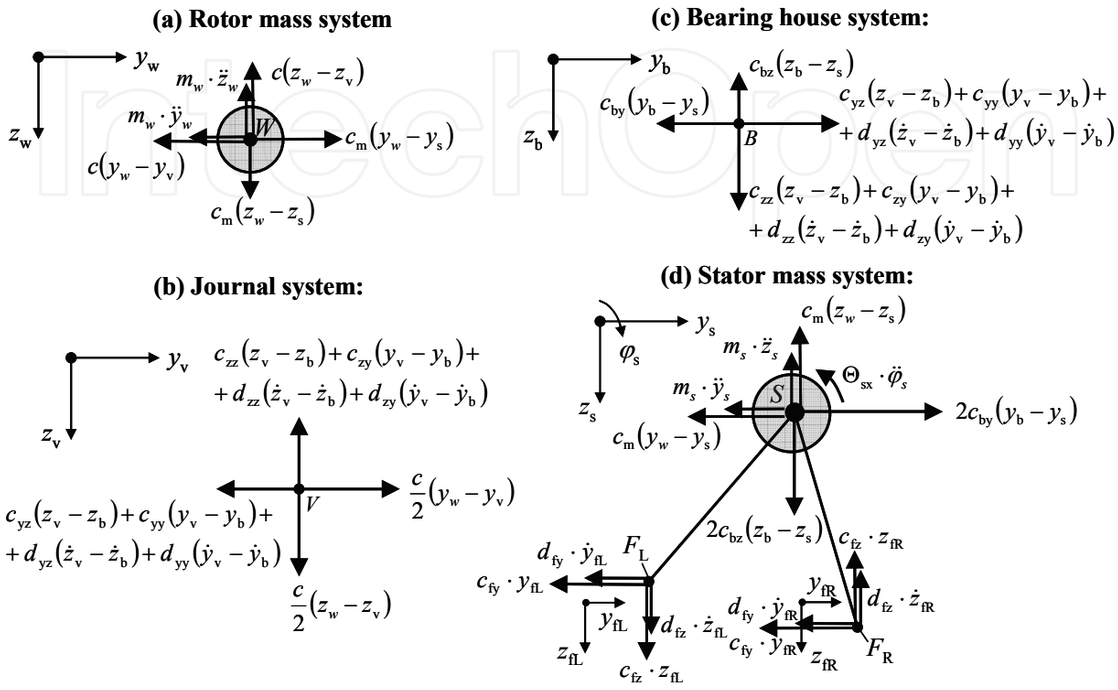

Fig. 4. Vibration system, split into four single systems

The equilibrium of forces and moments for each single system (Fig. 4) leads to following equations for each single system:

- Rotor mass system (Fig. 4a):

$$\uparrow: \qquad m_{\mathrm{w}} \cdot \ddot{z}_{\mathrm{w}} + c \cdot (z_{\mathrm{w}} - z_{\mathrm{v}}) - c_{\mathrm{m}} \cdot (z_{\mathrm{w}} - z_{\mathrm{s}}) = 0 \tag{2}$$

$$\rightarrow: \qquad m_{\mathrm{w}} \cdot \ddot{y}_{\mathrm{w}} + c \cdot (y_{\mathrm{w}} - y_{\mathrm{v}}) - c_{\mathrm{m}} \cdot (y_{\mathrm{w}} - y_{\mathrm{s}}) = 0 \tag{3}$$

- Journal system (Fig. 4b):

$$\uparrow: \qquad c_{zz}(z_{\mathrm{v}} - z_{\mathrm{b}}) + c_{zy}(y_{\mathrm{v}} - y_{\mathrm{b}}) + d_{zz}(\dot{z}_{\mathrm{v}} - \dot{z}_{\mathrm{b}}) + d_{zy}(\dot{y}_{\mathrm{v}} - \dot{y}_{\mathrm{b}}) - \frac{c}{2}(z_{\mathrm{w}} - z_{\mathrm{v}}) = 0 \tag{4}$$

$$\rightarrow: \qquad c_{yz}(z_{\mathrm{v}} - z_{\mathrm{b}}) + c_{yy}(y_{\mathrm{v}} - y_{\mathrm{b}}) + d_{yz}(\dot{z}_{\mathrm{v}} - \dot{z}_{\mathrm{b}}) + d_{yy}(\dot{y}_{\mathrm{v}} - \dot{y}_{\mathrm{b}}) - \frac{c}{2}(y_{\mathrm{w}} - y_{\mathrm{v}}) = 0 \tag{5}$$

- Bearing house system (Fig. 4c):

$$\uparrow: \qquad c_{zz}(z_{\mathrm{v}} - z_{\mathrm{b}}) + c_{zy}(y_{\mathrm{v}} - y_{\mathrm{b}}) + d_{zz}(\dot{z}_{\mathrm{v}} - \dot{z}_{\mathrm{b}}) + d_{zy}(\dot{y}_{\mathrm{v}} - \dot{y}_{\mathrm{b}}) - c_{\mathrm{bz}} \cdot (z_{\mathrm{b}} - z_{\mathrm{s}}) = 0 \tag{6}$$

$$\rightarrow: \qquad c_{yz}(z_{\mathrm{v}} - z_{\mathrm{b}}) + c_{yy}(y_{\mathrm{v}} - y_{\mathrm{b}}) + d_{yz}(\dot{z}_{\mathrm{v}} - \dot{z}_{\mathrm{b}}) + d_{yy}(\dot{y}_{\mathrm{v}} - \dot{y}_{\mathrm{b}}) - c_{\mathrm{by}} \cdot (y_{\mathrm{b}} - y_{\mathrm{s}}) = 0 \tag{7}$$

- Stator mass system (Fig. 4d):

$$\uparrow: \quad m_s \cdot \ddot{z}_s + c_m \cdot (z_w - z_s) - 2c_{bz} \cdot (z_b - z_s) + c_{fz} \cdot z_{fR} + d_{fz} \cdot \dot{z}_{fR} - c_{fz} \cdot z_{fL} - d_{fz} \cdot \dot{z}_{fL} = 0 \tag{8}$$

$$\rightarrow: \quad m_s \cdot \ddot{y}_s + c_m \cdot (y_w - y_s) - 2c_{by} \cdot (y_b - y_s) + c_{fy} \cdot y_{fR} + d_{fy} \cdot \dot{y}_{fR} + c_{fy} \cdot y_{fL} + d_{fy} \cdot \dot{y}_{fL} = 0 \tag{9}$$

$$S: \quad \Theta_{sx} \cdot \ddot{\varphi}_s + b \cdot (c_{fz} z_{fR} + d_{fz} \dot{z}_{fR} + c_{fz} z_{fL} + d_{fz} \dot{z}_{fL}) - h \cdot (c_{fy} y_{fR} + d_{fy} \dot{y}_{fR} + c_{fy} y_{fL} + d_{fy} \dot{y}_{fL}) = 0 \tag{10}$$

The equations (2)-(10) lead to a linear homogenous differential equation system (11) with 13 degrees of freedom (DOF = 13), with the mass matrix $\mathbf{M}_o$, the damping matrix $\mathbf{D}_o$ and the stiffness matrix $\mathbf{C}_o$, which have the form 13x13.

$$\mathbf{M}_o \cdot \ddot{\mathbf{q}}_o + \mathbf{D}_o \cdot \dot{\mathbf{q}}_o + \mathbf{C}_o \cdot \mathbf{q}_o = \mathbf{0} \tag{11}$$

The coordinate vector $\mathbf{q}_o$ is a vector with 13 rows described by:

$$\mathbf{q}_o = (z_s; z_w; y_s; y_w; \varphi_s; z_v; z_b; y_v; y_b; z_{fR}; z_{fL}; y_{fR}; y_{fL})^T \tag{12}$$

The linear homogenous differential equation system can be reduced into a system of 9 DOF, by considering the cinematic constraints between the stator mass and the machine feet.

3.2 Kinematic constraints between stator mass and machine feet

The kinematic constraints are derived for translation of the stator mass and for angular displacement of the stator mass and for the superposition of both.

3.2.1 Kinematic constraints for translation of the stator mass

If the stator mass centre *S* makes only a translation (z_s, y_s) without angular displacement ($\varphi_s = 0$) the kinematic constraints between stator mass centre S and the machine feet F_L and F_R can be described as follows:

$$z_{fL} = z_{fR} = z_s \,; \; y_{fL} = y_{fR} = y_s \tag{13}$$

3.2.2 Kinematic constraints for angular displacement of the stator mass

If the stator mass centre *S* only makes an angular displacement (φ_s) without translation ($z_s = y_s = 0$) the kinematic constraints between the angular displacement (φ_s) of the stator mass centre *S* and the translation of the machine feet F_L and F_R are shown in Fig. 5.
The displacements of the machine feet on the left side of the machine can be described as follows:

$$z_{fL} = -u_{fL} \cdot \sin\beta = -2 \cdot l \cdot \sin\left(\frac{\varphi_s}{2}\right) \cdot \sin\beta \tag{14}$$

$$y_{fL} = -u_{fL} \cdot \cos\beta = -2 \cdot l \cdot \sin\left(\frac{\varphi_s}{2}\right) \cdot \cos\beta \tag{15}$$

The angle β is described by:

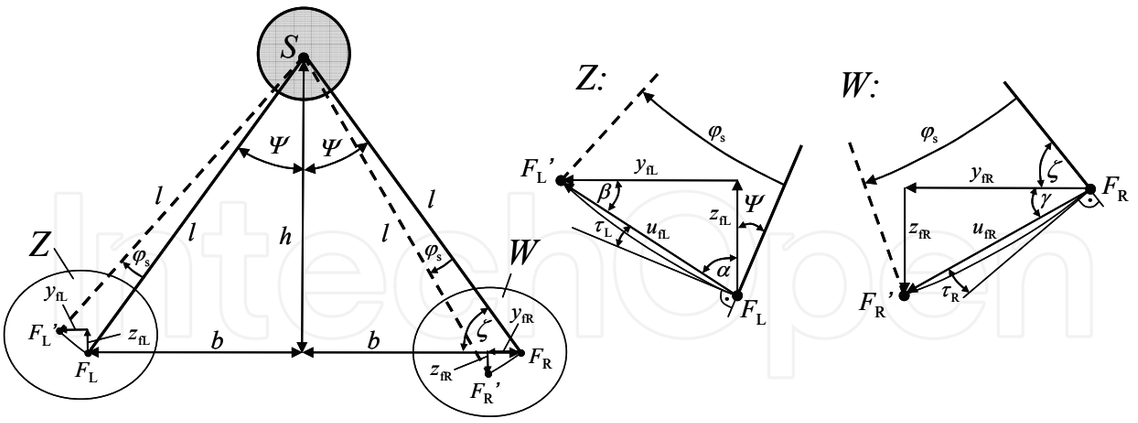

Fig. 5. Angular displacement φ_s of the stator mass centre S

$$\beta = 90° - \alpha = \tau_L + \Psi = \frac{\varphi_s}{2} + \Psi \tag{16}$$

The displacements of the machine feet on the right side of the machine can be described as follows:

$$z_{fR} = u_{fR} \cdot \sin\gamma = 2 \cdot l \cdot \sin\left(\frac{\varphi_s}{2}\right) \cdot \sin\gamma \tag{17}$$

$$y_{fR} = -u_{fR} \cdot \cos\gamma = -2 \cdot l \cdot \sin\left(\frac{\varphi_s}{2}\right) \cdot \cos\gamma \tag{18}$$

The angle γ is described by:

$$\gamma = 90° - \left(\zeta + \tau_R\right) = 90° - \left(\zeta + \frac{\varphi_s}{2}\right) \tag{19}$$

For small angular displacements φ_s of the stator mass centre S (φ_s << Ψ and φ_s << ζ) following linearizations can be deduced:

$$\sin\left(\frac{\varphi_s}{2}\right) \rightarrow \frac{\varphi_s}{2} \tag{20}$$

$$\beta = \frac{\varphi_s}{2} + \Psi \rightarrow \beta \approx \Psi \tag{21}$$

$$\gamma = 90° - \left(\zeta + \frac{\varphi_s}{2}\right) \rightarrow \gamma \approx 90° - \zeta \tag{22}$$

With these linearizations the displacements of the machine feet on the left side and on the right side can be described as follows:

$$z_{\mathrm{fL}} = -l \cdot \varphi_{\mathrm{s}} \cdot \sin\Psi = -b \cdot \varphi_{\mathrm{s}} \tag{23}$$

$$y_{\mathrm{fL}} = -l \cdot \varphi_{\mathrm{s}} \cdot \cos\Psi = -h \cdot \varphi_{\mathrm{s}} \tag{24}$$

$$z_{\mathrm{fR}} = l \cdot \varphi_{\mathrm{s}} \cdot \sin(90° - \zeta) = b \cdot \varphi_{\mathrm{s}} \tag{25}$$

$$y_{\mathrm{fR}} = -l \cdot \varphi_{\mathrm{s}} \cdot \cos(90° - \zeta) = -h \cdot \varphi_{\mathrm{s}} \tag{26}$$

3.2.3 Kinematic constraints for superposition of translation and angular displacement

For superposition of the translation and angular displacement of the stator mass centre S following kinematic constraints can be derived:

$$z_{\mathrm{fL}} = z_{\mathrm{s}} - b \cdot \varphi_{\mathrm{s}} \tag{27}$$

$$y_{\mathrm{fL}} = y_{\mathrm{s}} - h \cdot \varphi_{\mathrm{s}} \tag{28}$$

$$z_{\mathrm{fR}} = z_{\mathrm{s}} + b \cdot \varphi_{\mathrm{s}} \tag{29}$$

$$y_{\mathrm{fR}} = y_{\mathrm{s}} - h \cdot \varphi_{\mathrm{s}} \tag{30}$$

Therefore, it is possible to describe the translations of the machine feet (z_{fL}; y_{fL}; z_{fR}; y_{fR}) by the movement of the stator mass (z_{s}, y_{s}, φ_{s}).

3.3 Reduced homogenous differential equation system

With the kinematic constraints (27)-(30) the differential equation system (11) – with 13 DOF – can be reduced to a differential equation system of 9 DOF. By deriving the reduced differential equation system, it is necessary to consider, that the negative vertical displacement of the machine foot F_{L}, related to the coordinate system in Fig. 4 is considered in the direction of the vertical forces in F_{L}. Therefore the displacement z_{fL} has to be described negative $z_{\mathrm{fL}} \rightarrow -z_{\mathrm{fL}}$, as well as the velocity $\dot{z}_{\mathrm{fL}} \rightarrow -\dot{z}_{\mathrm{fL}}$. With this boundary condition and with the kinematic constraints (27)-(30) the equations for the stator system (8)-(10) become:

$$\uparrow: \quad m_{\mathrm{s}} \cdot \ddot{z}_{\mathrm{s}} + c_{\mathrm{m}} \cdot (z_{\mathrm{w}} - z_{\mathrm{s}}) - 2c_{\mathrm{bz}} \cdot (z_{\mathrm{b}} - z_{\mathrm{s}}) + 2c_{\mathrm{fz}} \cdot z_{\mathrm{s}} + 2d_{\mathrm{fz}} \cdot \dot{z}_{\mathrm{s}} = 0 \tag{31}$$

$$\rightarrow: \quad m_{\mathrm{s}} \cdot \ddot{y}_{\mathrm{s}} + c_{\mathrm{m}} \cdot (y_{\mathrm{w}} - y_{\mathrm{s}}) - 2c_{\mathrm{by}} \cdot (y_{\mathrm{b}} - y_{\mathrm{s}}) + 2c_{\mathrm{fy}} \cdot (y_{\mathrm{s}} - h \cdot \varphi_{\mathrm{s}}) + 2d_{\mathrm{fy}} \cdot (\dot{y}_{\mathrm{s}} - h \cdot \dot{\varphi}_{\mathrm{s}}) = 0 \tag{32}$$

$$\circlearrowright S: \quad \Theta_{\mathrm{sx}} \cdot \ddot{\varphi}_{\mathrm{s}} - 2d_{\mathrm{fy}} h \cdot \dot{y}_{\mathrm{s}} + 2(d_{\mathrm{fy}} h^2 + d_{\mathrm{fz}} b^2) \cdot \dot{\varphi}_{\mathrm{s}} - 2c_{\mathrm{fy}} h \cdot y_{\mathrm{s}} + 2(c_{\mathrm{fy}} h^2 + c_{\mathrm{fz}} b^2) \cdot \varphi_{\mathrm{s}} = 0 \tag{33}$$

Therefore, it is now possible to derive the reduced homogenous differential equation system, which only has 9 DOF:

$$\mathbf{M} \cdot \ddot{\mathbf{q}} + \mathbf{D} \cdot \dot{\mathbf{q}} + \mathbf{C} \cdot \mathbf{q} = \mathbf{0} \tag{34}$$

The mass matrix **M** and coordinate vector **q** are described by:

$$\mathbf{M}=\begin{pmatrix} m_{\mathrm{s}} & 0 & 0 & 0 & 0 & 0 & 0 & 0 & 0 \\ 0 & m_{\mathrm{w}} & 0 & 0 & 0 & 0 & 0 & 0 & 0 \\ 0 & 0 & m_{\mathrm{s}} & 0 & 0 & 0 & 0 & 0 & 0 \\ 0 & 0 & 0 & m_{\mathrm{w}} & 0 & 0 & 0 & 0 & 0 \\ 0 & 0 & 0 & 0 & \Theta_{\mathrm{sx}} & 0 & 0 & 0 & 0 \\ 0 & 0 & 0 & 0 & 0 & 0 & 0 & 0 & 0 \\ 0 & 0 & 0 & 0 & 0 & 0 & 0 & 0 & 0 \\ 0 & 0 & 0 & 0 & 0 & 0 & 0 & 0 & 0 \\ 0 & 0 & 0 & 0 & 0 & 0 & 0 & 0 & 0 \end{pmatrix} \quad ; \quad \mathbf{q}=\begin{pmatrix} z_{\mathrm{s}} \\ z_{w} \\ y_{\mathrm{s}} \\ y_{w} \\ \varphi_{\mathrm{s}} \\ z_{\mathrm{v}} \\ z_{\mathrm{b}} \\ y_{\mathrm{v}} \\ y_{\mathrm{b}} \end{pmatrix} \tag{35}$$

The damping matrix **D** is described by:

$$\mathbf{D}=\begin{pmatrix} 2d_{\mathrm{fz}} & 0 & 0 & 0 & 0 & 0 & 0 & 0 & 0 \\ 0 & 0 & 0 & 0 & 0 & 0 & 0 & 0 & 0 \\ 0 & 0 & 2d_{\mathrm{fy}} & 0 & -2d_{\mathrm{fy}}h & 0 & 0 & 0 & 0 \\ 0 & 0 & 0 & 0 & 0 & 0 & 0 & 0 & 0 \\ 0 & 0 & -2d_{\mathrm{fy}}h & 0 & 2\left(d_{\mathrm{fy}}h^2+d_{\mathrm{fz}}b^2\right) & 0 & 0 & 0 & 0 \\ 0 & 0 & 0 & 0 & 0 & 2d_{zz} & -2d_{zz} & 2d_{zy} & -2d_{zy} \\ 0 & 0 & 0 & 0 & 0 & -2d_{zz} & 2d_{zz} & -2d_{zy} & 2d_{zy} \\ 0 & 0 & 0 & 0 & 0 & 2d_{\mathrm{yz}} & -2d_{\mathrm{yz}} & 2d_{\mathrm{yy}} & -2d_{\mathrm{yy}} \\ 0 & 0 & 0 & 0 & 0 & -2d_{\mathrm{yz}} & 2d_{\mathrm{yz}} & -2d_{\mathrm{yy}} & 2d_{\mathrm{yy}} \end{pmatrix} \tag{36}$$

The stiffness matrix **C** is described by:

$$\mathbf{C}=\begin{pmatrix} 2(c_{\mathrm{fz}}+c_{\mathrm{bz}})-c_{\mathrm{m}} & c_{\mathrm{m}} & 0 & 0 & 0 & 0 & -2c_{\mathrm{bz}} & 0 & 0 \\ c_{\mathrm{m}} & c-c_{\mathrm{m}} & 0 & 0 & 0 & -c & 0 & 0 & 0 \\ 0 & 0 & 2(c_{\mathrm{fy}}+c_{\mathrm{by}})-c_{\mathrm{m}} & c_{\mathrm{m}} & -2c_{\mathrm{fy}}h & 0 & 0 & 0 & -2c_{\mathrm{by}} \\ 0 & 0 & c_{\mathrm{m}} & c-c_{\mathrm{m}} & 0 & 0 & 0 & -c & 0 \\ 0 & 0 & -2c_{\mathrm{fy}}h & 0 & 2\left(c_{\mathrm{fy}}h^2+c_{\mathrm{fz}}b^2\right) & 0 & 0 & 0 & 0 \\ 0 & -c & 0 & 0 & 0 & 2c_{zz}+c & -2c_{zz} & 2c_{zy} & -2c_{zy} \\ -2c_{\mathrm{bz}} & 0 & 0 & 0 & 0 & -2c_{zz} & 2(c_{zz}+c_{\mathrm{bz}}) & -2c_{zy} & 2c_{zy} \\ 0 & 0 & 0 & -c & 0 & 2c_{\mathrm{yz}} & -2c_{\mathrm{yz}} & 2c_{\mathrm{yy}}+c & -2c_{\mathrm{yy}} \\ 0 & 0 & -2c_{\mathrm{by}} & 0 & 0 & -2c_{\mathrm{yz}} & 2c_{\mathrm{yz}} & -2c_{\mathrm{yy}} & 2(c_{\mathrm{yy}}+c_{\mathrm{by}}) \end{pmatrix} \tag{37}$$

3.4 Solution of the reduced homogenous differential equation system

The natural vibrations can be derived by solving the homogeneous differential equation (34). Therefore usually a complex ansatz is used. So the homogeneous differential equation is described complex, with the vector $\underline{\mathbf{q}}$ as a complex vector (underlined = complex value), the mass matrix **M**, the damping matrix **D** and the stiffness matrix **C**.

$$\mathbf{M}\cdot\ddot{\underline{\mathbf{q}}}+\mathbf{D}\cdot\dot{\underline{\mathbf{q}}}+\mathbf{C}\cdot\underline{\mathbf{q}}=\mathbf{0} \quad \text{with: } \underline{\mathbf{q}}=(\underline{z}_{\mathrm{s}};\underline{z}_{\mathrm{w}};\underline{y}_{\mathrm{s}};\underline{y}_{\mathrm{w}};\underline{\varphi}_{\mathrm{s}};\underline{z}_{\mathrm{v}};\underline{z}_{\mathrm{b}};\underline{y}_{\mathrm{v}};\underline{y}_{\mathrm{b}})^{T} \tag{38}$$

The complex ansatz – with the complex eigenvalue $\underline{\lambda}$ and the complex eigenvectors $\underline{\hat{\mathbf{q}}}$ –

$$\underline{\mathbf{q}} = \underline{\hat{\mathbf{q}}} \cdot e^{\underline{\lambda} \cdot t} \quad \text{with:} \quad \underline{\hat{\mathbf{q}}} = (\underline{\hat{z}}_s ; \underline{\hat{z}}_w ; \underline{\hat{y}}_s ; \underline{\hat{y}}_w ; \underline{\hat{\varphi}}_s ; \underline{\hat{z}}_v ; \underline{\hat{z}}_b ; \underline{\hat{y}}_v ; \underline{\hat{y}}_b)^T \tag{39}$$

leads to the eigenvalue equation:

$$[\mathbf{C} + \underline{\lambda} \cdot \mathbf{D} + \underline{\lambda}^2 \cdot \mathbf{M}] \cdot \underline{\hat{\mathbf{q}}} = \mathbf{0} \tag{40}$$

To get the complex eigenvalues $\underline{\lambda}$, it is necessary to solve the determination equation:

$$\det[\mathbf{C} + \underline{\lambda} \cdot \mathbf{D} + \underline{\lambda}^2 \cdot \mathbf{M}] = 0 \tag{41}$$

This leads to a characteristic polynomial of 12th grade:

$$\sum_{n=0}^{12} A_n \cdot \underline{\lambda}^n = 0 \tag{42}$$

With a numerical solution of this polynomial, n complex eigenvalues $\underline{\lambda}_n$ – with the real parts α_n, which describe the decay of each natural vibration and the imaginary parts ω_n, which describe the corresponding natural angular frequencies – can be calculated. The eigenvalues occur mostly conjugated complex (j: imaginary unit $\rightarrow j^2 = -1$):

$$\underline{\lambda}_n = \alpha_n \pm j \cdot \omega_n \tag{43}$$

With the complex eigenvalues $\underline{\lambda}_n$ the complex eigenvectors $\underline{\hat{\mathbf{q}}}_n$ can be calculated. Therefore the natural vibrations can be described by:

$$\underline{\mathbf{q}} = \sum_{n=1}^{12} \underline{\hat{\mathbf{q}}}_n \cdot \underline{k}_n \cdot e^{\underline{\lambda}_n \cdot t} \tag{44}$$

The factors $\underline{k}_n$ can be used, to adapt the natural vibrations to the starting conditions. Using the calculated real part α_n and the imaginary part ω_n of each complex eigenvalue λ_n the modal damping D_n of each natural vibration mode can be derived (Kellenberger, 1987).

$$D_n = \frac{-\alpha_n}{\sqrt{\alpha_n^2 + \omega_n^2}} \tag{45}$$

3.5 Stability of the vibration system

If the oil film stiffness matrix $\mathbf{C}_v$ of the sleeve bearings is non symmetric ($c_{zy} \neq c_{yz}$) – for e.g. sleeve bearings with cylindrical shell the cross-coupling coefficients of the stiffness matrix are mostly unequal ($c_{zy} \neq c_{yz}$) – also the system stiffness matrix $\mathbf{C}$ (37) gets non symmetric. This may lead to instabilities of the vibration system (Gasch et al., 2002), which occur if the real part of one or more complex eigenvalues gets positive, leading to negative modal damping values (45). The oil film stiffness and damping coefficients are a function of the rotary angular frequency Ω of the rotor.

$$c_{ij} = c_{ij}(\Omega) \; ; \quad d_{ij} = d_{ij}(\Omega) \quad \text{with} \quad i, j = z, y \tag{46}$$

To find the limit of stability of the vibration system, the rotary angular frequency Ω has to be increased, until the real part of one or more complex eigenvalues becomes zero. Then the limit of stability is reached at the rotary angular frequency $\Omega = \Omega_{\text{limit}}$. At the limit of stability the natural angular frequency of the critical mode becomes ω_{limit} and no damping exists ($\alpha_{\text{limit}} = 0$). So the critical complex eigenvalue at the limit of stability becomes:

$$\underline{\lambda}_{\text{limit}} = \pm j \cdot \omega_{\text{limit}} \quad \text{with } \alpha_{\text{limit}} = 0 \tag{47}$$

With this complex eigenvalue the complex eigenvector can be calculated. So the undamped natural vibration at the limit of stability can be described by:

$$\underline{\mathbf{q}}_{\text{limit}} = \underline{\hat{\mathbf{q}}}^{+}_{\text{limit}} \cdot \underline{k}^{+}_{\text{limit}} \cdot e^{j\omega_{\text{limit}} \cdot t} + \underline{\hat{\mathbf{q}}}^{-}_{\text{limit}} \cdot \underline{k}^{-}_{\text{limit}} \cdot e^{-j\omega_{\text{limit}} \cdot t} \tag{48}$$

At the limit of stability, that means at the rotary angular frequency of Ω_{limit}, which represents the rotor speed n_{limit} ($= \Omega_{\text{limit}}/2\pi$), the undamped mode (with $\alpha_{\text{limit}} = 0$) oscillates with the natural angular frequency of ω_{limit}, as a self exciting vibration.

4. Example

In this chapter the natural frequencies of a 2-pole induction motor (Fig. 1), mounted on a rigid foundation and also mounted on a soft steel frame foundation, is analyzed.

4.1 Data of motor, sleeve bearing and foundation

The machine data, sleeve bearing data and foundation data are shown in Table 1. First the stiffness data of the foundation are chosen arbitrarily. The damping ratio D_f of the steel frame foundation is assumed to be 0.02, which is common for a welded steel frame.

Machine data		**Sleeve bearing data**	
Rated power	P_N = 2000 kW	Type of bearing	Side flange bearing
Number of pole pairs	p = 1	Bearing shell	Cylindrical
Rated voltage	U_N = 6000 V	Lubricant viscosity grade	ISO VG 32
Rated frequency	f_N = 50 Hz	Nominal bore diameter	d_b = 110 mm
Rated torque	M_N = 6.4 kNm	Bearing width	b_b = 81.4 mm
Rated speed	n_N = 2990 r/min	Ambient temperature	T_{amb} = 25°C
Mass of the stator	m_s = 7200 kg	Lubricant supply temp.	T_{in} = 40°C
Mass of the rotor	m_w = 1900 kg	Mean relative bearing clearance (DIN 31698)	Ψ_m = 1.6 ‰
Moment of inertia of the stator	Θ_{sx} = 1550 kgm²		
Height of the centre of gravity	h = 560 mm	**Foundation data**	
Distance between feet	$2b$ = 1060 mm		
Rotor stiffness	c = 155.7 kN/mm	Vertical foundation stiffness at each motor side	c_{fz} = 133 kN/mm
Magnetic spring constant	c_m = 7.15 kN/mm	Horizontal foundation stiffness at each motor side	c_{fy} = 100 kN/mm
Vertical stiffness of bearing house and end shield	c_{bz} = 570 kN/mm	Damping ratio of the steel frame foundation	D_f = 0.02
Horizontal stiffness of bearing house and end shield	c_{by} = 480 kN/mm		

Table 1. Data of induction motor, sleeve bearings and foundation

4.2 Oil film stiffness and damping coefficients

The oil film stiffness and damping coefficients of the sleeve bearings are calculated for each rotor speed in steady state operation, using the program SBCALC from RENK AG.

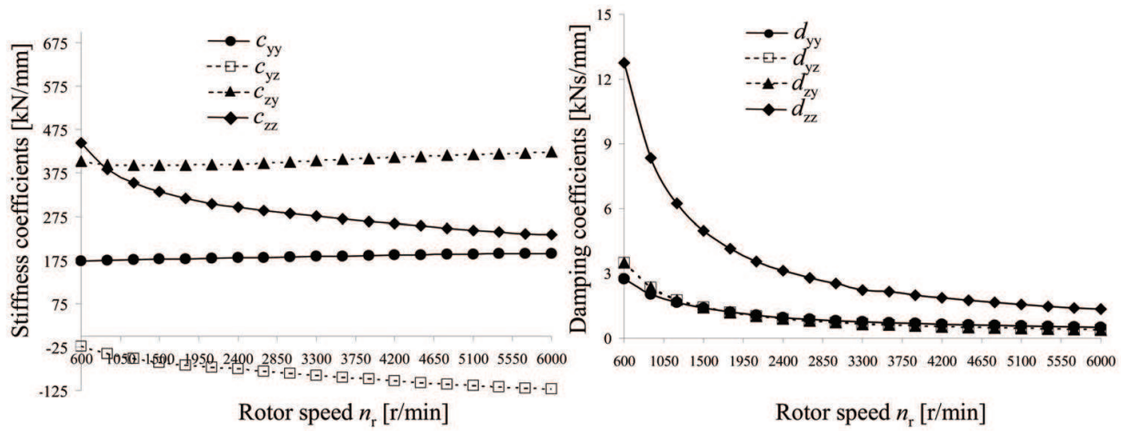

Fig. 6. Oil film stiffness and damping coefficients for different rotor speeds

4.3 Used FE-Program

To calculate the natural vibrations and to picture the mode shapes the finite element program MADYN is used. A simplified finite element model is used (Fig. 7), which is based on the model in Fig. 2. The degrees of freedom of the nodes are chosen in such a way, that only movements in the transversal plane (*y*-*z* plane) occur.

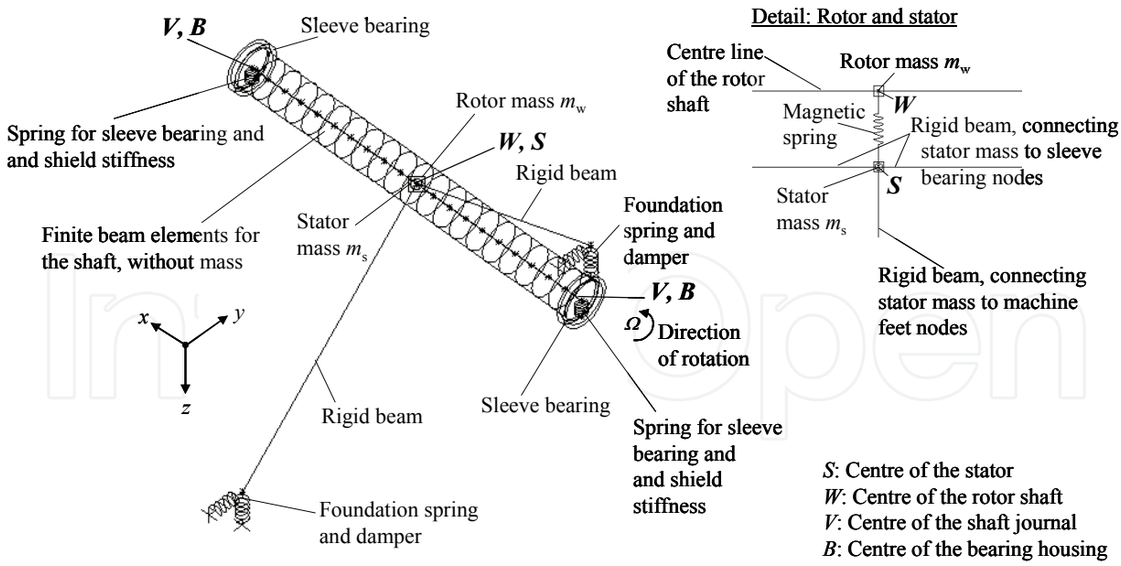

Fig. 7. Finite element model

Additionally the analytical formulas from chapter 3 could be validated with this finite element model, by comparing the calculated eigenvalues, calculated by the analytical formulas – which were solved by using the mathematic program MATHCAD – with the eigenvalues, calculated with the finite element program MADYN.

4.4 Natural vibrations; motor mounted on a rigid foundation

Before the natural vibrations of the motor, mounted on the soft steel frame foundation, are analyzed the natural vibrations of the motor, mounted on a rigid foundation are calculated. Therefore the foundation stiffness values are assumed to be infinite high ($c_{fz} = c_{yz} \rightarrow \infty$).

4.4.1 Natural vibrations at rated speed

First the natural vibrations at rated speed are calculated. The mode shapes are pictured in Fig. 8. In the 1st mode the rotor mass – shaft centre point *W* - moves on an elliptical orbit, which is run through forwards. The semi-major axis of the orbit is about 34° shifted out of the horizontal axis. The orbit of rotor mass is larger than the orbits of the shaft journals. The orbits of the shaft journals – shaft journal points *V* – have the same orientation as the orbit of the rotor mass and are also run through forwards. The orbits of the bearing housing points *B* are much smaller than the orbits of the shaft journal points *V*, but are also run through forwards. Their semi-major axes are about 28° shifted out of the horizontal axis. Because of the infinite stiffness of the foundation no movement of the stator mass occurs. In the 2nd mode the semi-major axes of all orbits have the nearly the same orientation, shifted about 8° out of the horizontal axis. All orbits are run through forwards. In this mode the largest orbits are the orbits of the shaft journal points *V*. In the 3rd mode the semi-major axes of the

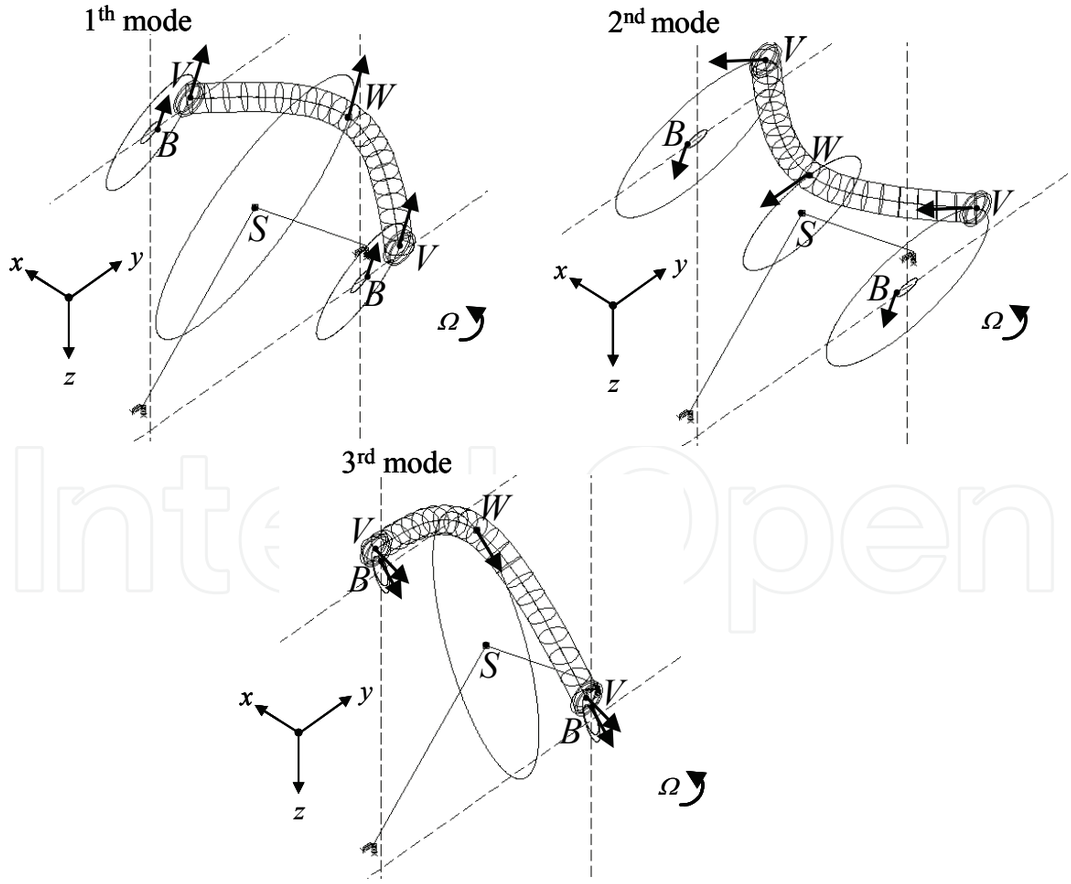

Fig. 8. Mode shapes, motor mounted on a rigid foundation, operating at rated speed (n_N = 2990 r/min)

shaft centre point W and of the shaft journal points V are shifted about 15° out of the vertical axis. The semi-major axes of the bearing housing points B are shifted about 20° out of the vertical axis. All orbits are run through backwards. In this mode the orbit of the shaft centre point W is much larger than the orbits of the shaft journal points V and the orbits of the bearing housing points B, which are nearly equal to each other. This leads to a strong bending of the rotor shaft with only small orbits in the sleeve bearings.
The natural frequencies and the modal damping values are shown in Table 2. Because of the assumption of an infinite high foundation stiffness ($c_{fz} = c_{yz} \rightarrow \infty$) only three natural vibrations occur with three natural frequencies f_1, f_2, f_3 and three modal damping values D_1, D_2,D_3. The modal damping values are here described in percentage.

Modes n	Natural frequency f_n [Hz]	Modal damping D_n[%]
1	33.15	5.31
2	34.62	68.24
3	41.17	3.82

Table 2. Natural frequencies and modal damping, motor mounted on a rigid foundation, operating at rated speed (n_N = 2990 r/min)

4.4.2 Critical speed map

In this chapter the natural frequencies and the modal damping for different rotor speeds are calculated and a critical speed map is derived (Fig. 9).
Fig. 9 shows how the natural frequencies f_n and the modal damping values D_n change with the rotor speed n_r, caused by the changing of the oil film stiffness and damping coefficients. Where the rotary frequency ($\Omega/2\pi$) meets the natural frequencies critical speeds regarding the 1x excitation may occur if the modal damping value is low at this rotor speed. Usually, if the modal damping value D_n is higher than 20% no critical resonance vibrations are expected and the rotor speed is usually not assumed to be a critical speed. Here two critical speeds have to be passed to reach the operating speed. The 1st critical speed occurs at about a rotor speed of 2070 r/min with a modal damping value of about 15%. The 2nd critical speed occurs at a rotor speed of 2475 r/min with a modal damping value of about 3.5%. Fig. 9 shows that a separation margin larger than 15% for the critical speeds to the operating speed (2990 r/min) is given, which is required in many standards and specifications. Fig. 9 shows additionally that limit of stability is reached at a rotor speed of about 3900 r/min. Here the modal damping of mode 1 gets zero.

4.4.3 Stiffness variation map regarding the electromagnetic stiffness

In this chapter the influence of the electromagnetic stiffness between the rotor and the stator on the natural frequencies is analyzed. Therefore the magnetic spring constant c_m, which describes the electromagnetic stiffness between rotor and stator, is variegated by a factor k_{cm}, called magnetic stiffness factor. The rated magnetic spring constant is $c_{m,rated}$ = 7.15 kN/mm (Table 1). The magnetic stiffness factor k_{cm} is variegated in the range of 0…2 and the influence on the natural frequencies and modal damping values are calculated for operation at rated speed (Fig. 10).

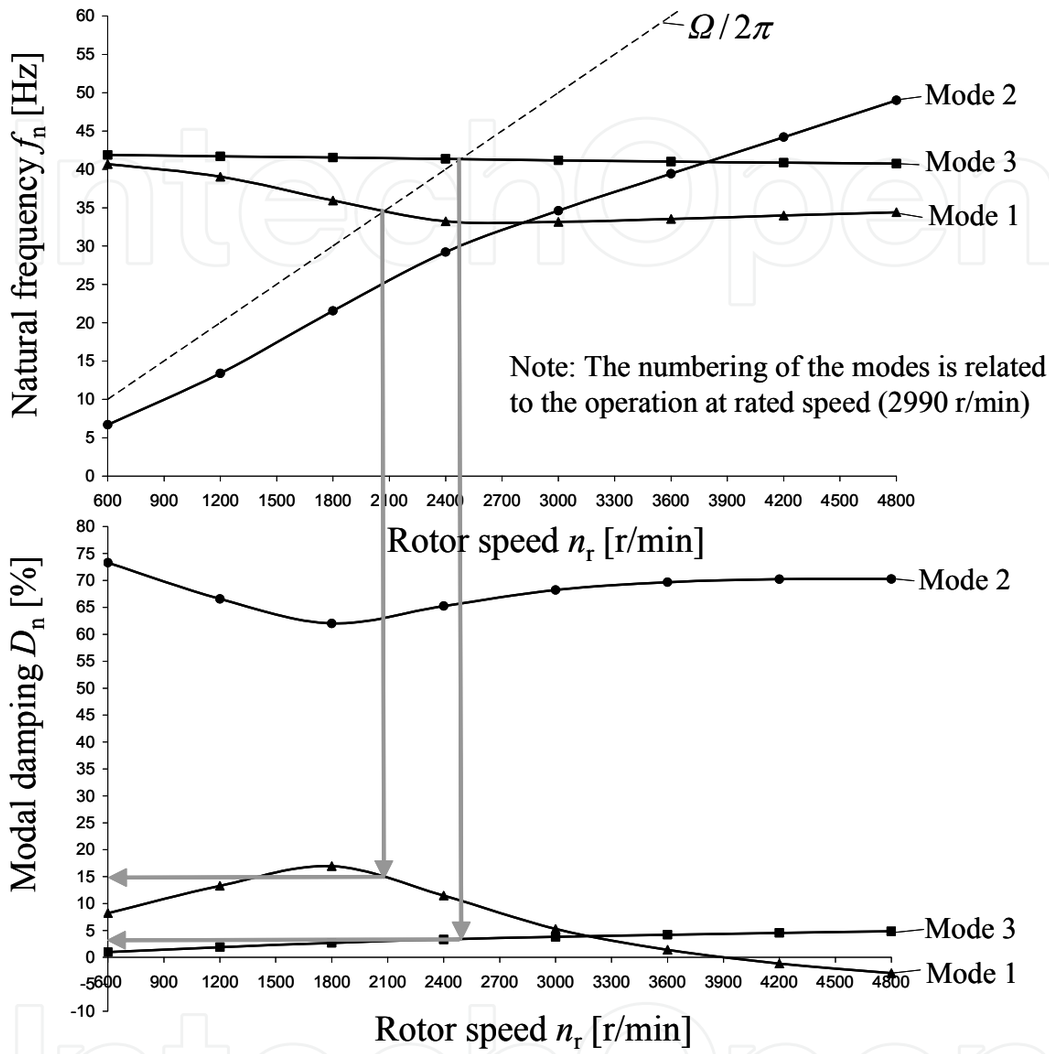

Fig. 9. Critical speed map, motor mounted on a rigid foundation

$$\text{Magnetic spring constant:} \qquad c_m = k_{cm} \cdot c_{m,rated} \tag{49}$$

Fig. 10 shows that mode 1 and mode 3 are clearly influenced by the magnetic spring constant. Their natural frequencies and modal damping values change with the magnetic stiffness factor, whereas mode 2 is hardly influenced by the magnetic spring value. The reason is that the orbits of rotor mass are larger than the orbits of the shaft journals for mode 1 and mode 3 (Fig. 8), contrarily to mode 2, where the orbits of the shaft journals are larger. Therefore the influence of the magnetic spring constant, which acts at the rotor mass, is higher for mode 1 and mode 3.

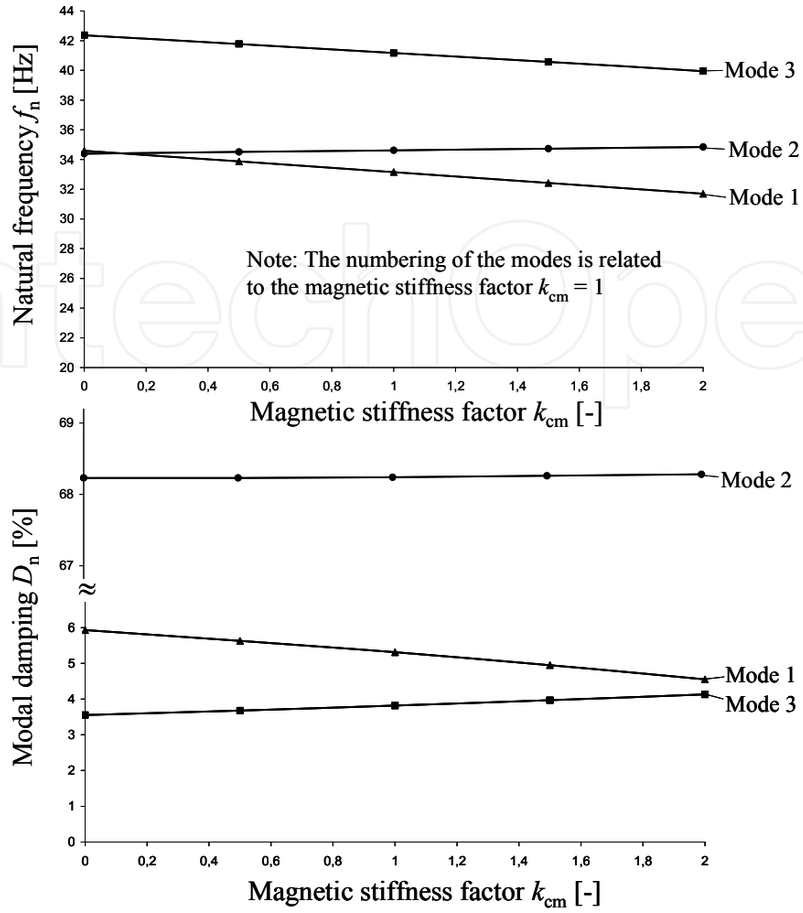

Fig. 10. Stiffness variation map regarding the electromagnetic stiffness, motor mounted on a rigid foundation, operating at rated speed (n_N = 2990 r/min)

4.5 Natural vibrations; motor mounted on a soft steel frame foundation

After the natural vibrations of the rigid mounted motor are analyzed, the natural vibrations of the motor, mounted on a soft steel frame foundation, are now investigated. The foundation data are described in Table 1.

4.5.1 Natural vibrations at rated speed

Again, the natural vibrations at rated speed are calculated first. The natural frequencies are calculated once without considering of the foundation damping (D_f = 0) and once with considering of the foundation damping (D_f = 0.02). The mode shapes without considering foundation damping are pictured in Fig. 11, which can be assumed to be equal to the mode shapes with considering foundation damping.

The first two modes are nearly rigid body modes of the soft mounted machine. Rotor and stator are nearly acting like a one-mass system. The orbits of the rotor and of the stator are nearly straight lines. In the 1st mode the rotor mass and the stator mass oscillate in phase to each other nearly in horizontal direction, while stator mass makes a lateral buckling at the x-axis, in the same direction as its horizontal movement. In the 2nd mode the rotor mass and the stator mass also oscillate in phase to each other, but in vertical direction. Nearly no buckling of

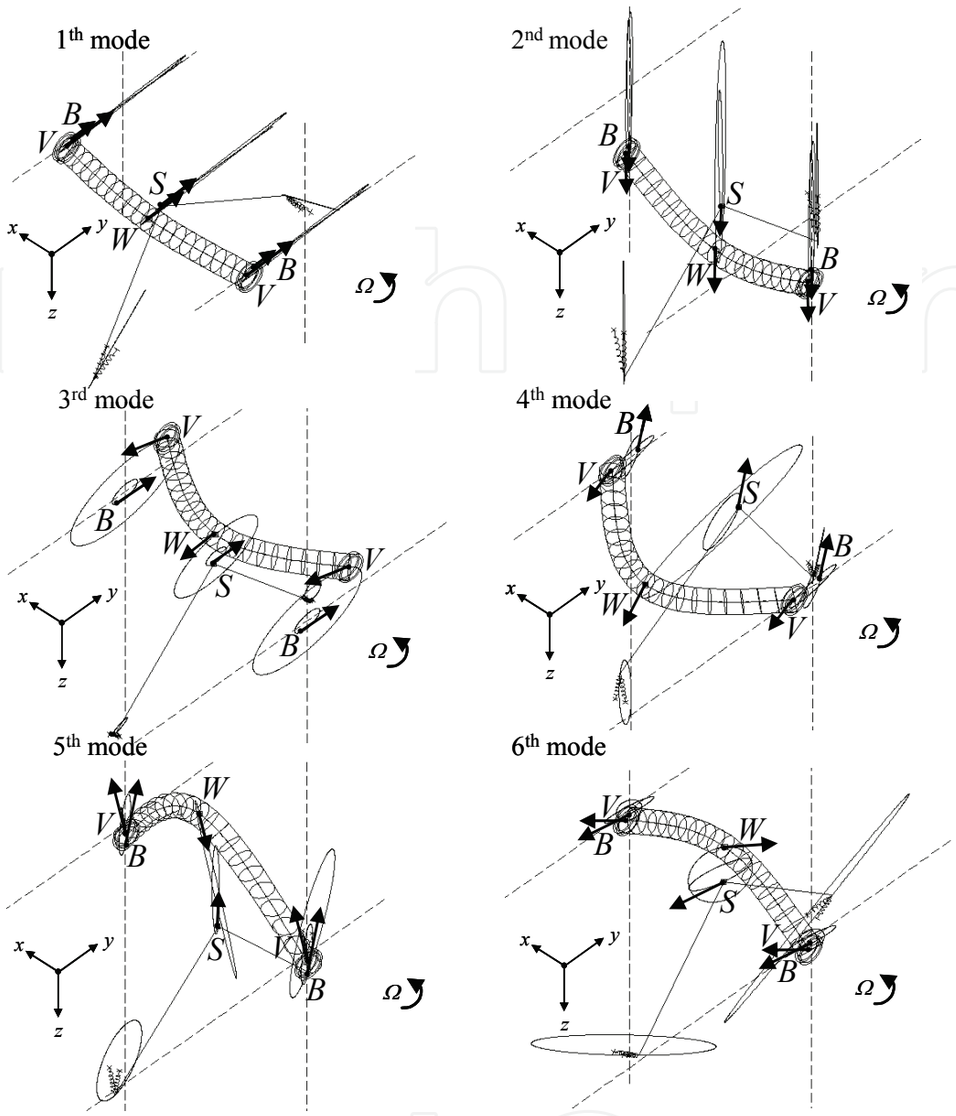

Fig. 11. Mode shapes, motor mounted on a soft steel frame foundation (c_{fz} = 133 kN/mm; c_{fy} = 100 kN/mm), without considering foundation damping (D_f =0), operating at rated speed (n_N = 2990 r/min)

the stator mass occurs. For the higher modes stator and rotor behave like a two- mass system and elliptical orbits of the rotor mass and stator mass occur. In the 3th mode the semi-major axes of orbits of the rotor mass, the bearing housings and the shaft journals are shifted about 12° out of the horizontal axis, whereas the semi-major axis of the orbit of the stator mass is only shifted 5° out of the horizontal axis. All orbits are run through forwards. The rotor mass and the stator mass oscillate out of phase to each other, as well as the shaft journals to the bearing housings. The largest orbits are the orbits of the shaft journals, compared to the other orbits. Because of the large relative orbits between the shaft journals and the bearing housings, the modal damping of this mode is very high, due to the oil film damping of the sleeve bearings. In the 4th mode the semi-major axis of the orbit of the rotor mass is shifted about 14° out of the horizontal axis. The same is valid for the shaft journals, whereas the semi-major axis of the

stator orbit is shifted about 47° out of the horizontal axis. The semi-major axes of the orbits of the bearing housings are shifted about 62° out of the horizontal axis. All orbits are still run through forwards. In the 5th mode the semi-major axis of the orbit of the rotor mass is shifted about 12° out of the vertical axis. The other orbits lie nearly in vertical direction. The stator mass and the rotor mass oscillate out of phase to each other. The orbit of the stator mass and the orbits of the bearing housing are run through forwards, while the orbit of the rotor mass and the orbits of the shaft journals are run through backwards. In the 6th mode the semi-major axes of the orbits of the stator mass and of the bearing housings are shifted about 80° out of the vertical axis, while the semi-major axes of the orbits of the rotor mass and of the shaft journals are shifted about 45° out of the vertical axis. All orbits are run through backwards. Additionally the 6th mode shows a strong lateral buckling of the stator mass at the x-axis, which leads to large orbits at the motor feet. Contrarily to the 1st mode the lateral buckling of the stator mass is contrariwise to its horizontal movement, which means that if the stator mass moves to the right the lateral buckling is to the left. To consider the influence of the foundation damping on the natural vibrations, a simplified approach is used. Referring to (Gasch et al., 2002), the damping ratio D_f of the foundation can be described by the damping coefficients d_{fq}, stiffness coefficients c_{fq} of the foundation and the stator mass m_s, as a rough simplification.

$$d_{fq} = D_f \cdot m_s \cdot \sqrt{2 \cdot c_{fq} / m_s} \quad \text{with: } q = z,y \tag{50}$$

The calculated natural frequencies and modal damping of each mode shape with and without considering foundation damping are shown in Table 3. It is shown that considering the foundation damping influences the natural frequencies only marginal, as expected. But the modal damping values of some modes are strongly influenced by the foundation damping. The modal damping values of the first two modes are strongly influenced by the foundation damping, because the modes are nearly rigid body modes of the motor on the foundation. Also the modal damping of the 6th mode is strongly influenced by the foundation damping, because large orbits of the motor feet occur in this mode shape, compared to the other orbits.

Modes n	Without foundation damping ($D_f = 0$)		With foundation damping ($D_f = 0.02$)	
	Natural frequency f_n [Hz]	Modal damping D_n [%]	Natural frequency f_n [Hz]	Modal damping D_n [%]
1	16.05	-0.11	16.05	0.95
2	25.35	0.51	25.33	1.84
3	35.22	65.75	35.23	65.72
4	37.72	6.97	37.67	7.36
5	48.50	3.39	48.54	4.24
6	52.63	1.0	52.61	4.17

Table 3. Natural frequencies and modal damping, motor mounted on a soft steel frame foundation (c_{fz} = 133 kN/mm; c_{fy} = 100 kN/mm) with and without considering foundation damping (D_f = 0.02 and D_f = 0), operating at rated speed (n_N = 2990 r/min)

4.5.2 Critical speed map

Again, a critical speed map is derived to show the influence of the rotor speed on the natural frequencies and the modal damping and to derive the critical speeds (Fig. 12).

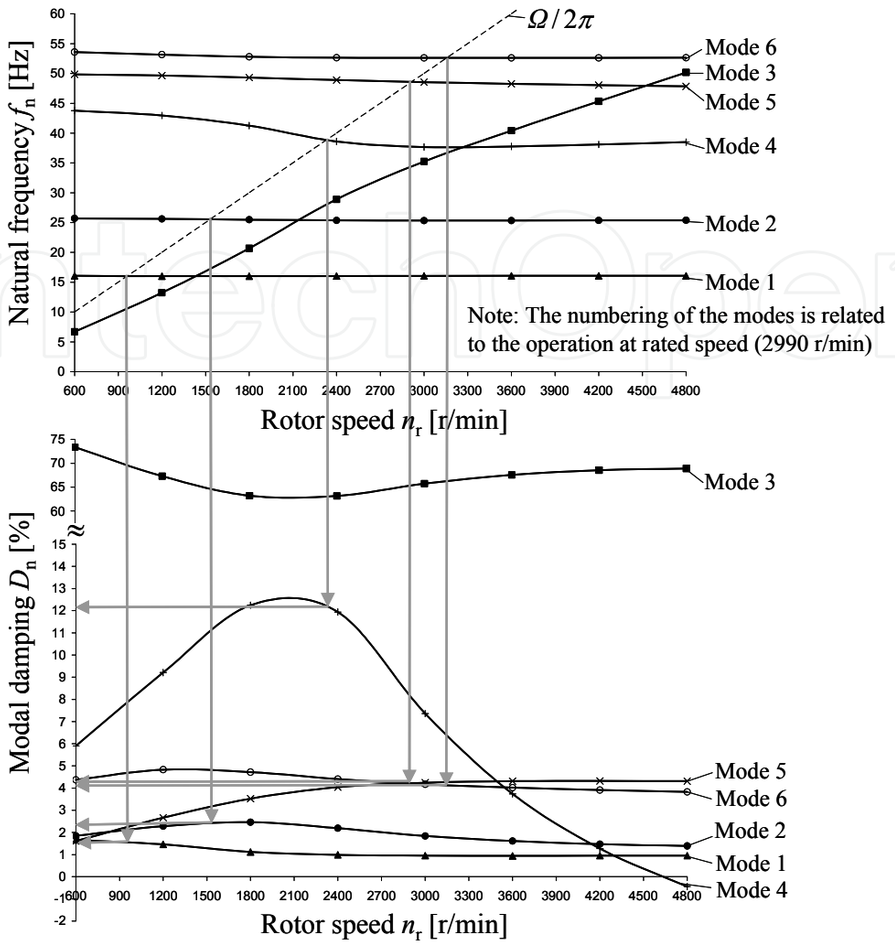

Fig. 12. Critical speed map, motor mounted on a soft steel frame foundation (c_{fz} = 133 kN/mm; c_{fy} = 100 kN/mm; D_f =0.02)

Critical speed	Critical speed [r/min]	Modal damping D_n [%]
1	950	1.6
2	1540	2.3
3	2340	12.2
4	2900	4.3
5	3160	4.2

Table 4. Critical speeds, motor mounted on a soft steel frame foundation (c_{fz} = 133 kN/mm; c_{fy} = 100 kN/mm; D_f =0.02)

Fig. 12 shows that the limit of stability is here reached at about 4650 r/min, because the modal damping of mode 4 gets zero at this rotor speed. For the rigid foundation the limit of stability is already reached at a rotor speed of about 3900 r/min. But contrarily to the rigid mounted motor here four critical speeds have to be passed before the operating speed (2990 r/min) is reached. Additionally a 5th critical speed is close above the operating speed. The critical speeds and the modal damping in the critical speeds are shown in Table 4.

Table 4 shows that two critical speeds (4th and 5th) with low modal damping values are very close to the operating speed (2990 r/min), having less than 5% separation margin to the operating speed. Therefore resonance vibrations problems may occur. The conclusion is that the arbitrarily chosen foundation stiffness values are not suitable for that motor with a operation speed of 2990 r/min. To find adequate foundation stiffness values, a stiffness variation of the foundation is deduced and a stiffness variation map is created (chapter 4.5.4). But preliminarily the influence of the electromagnetic stiffness on the natural frequencies and modal damping values is investigated for the soft mounted motor.

4.5.3 Stiffness variation map regarding the electromagnetic stiffness

In this chapter the influence of the electromagnetic stiffness on the natural frequencies and the modal damping values at rated speed is analyzed again, but now for the soft mounted motor. Again the magnetic stiffness factor k_{cm} is variegated in a range of 0….2 and the influence on the natural frequencies and the modal damping values is analyzed. Fig. 13

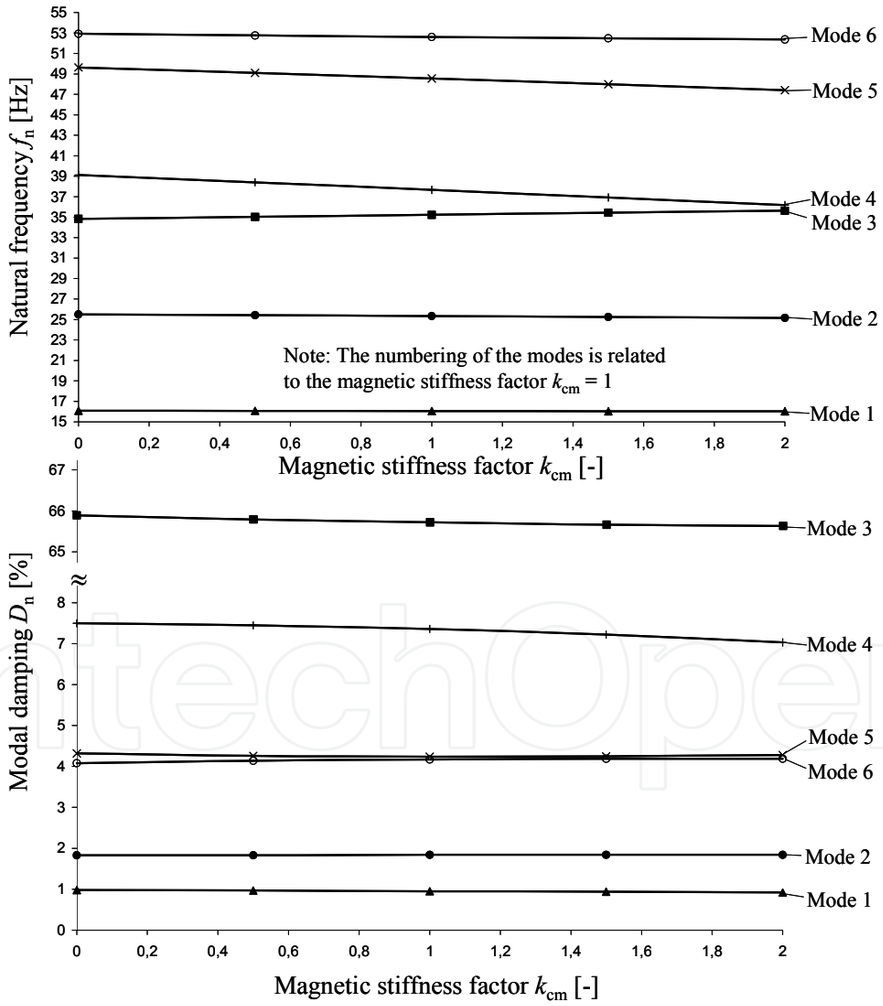

Fig. 13. Stiffness variation map regarding the electromagnetic stiffness, motor mounted on a soft steel frame foundation (c_{fz} = 133 kN/mm; c_{fy} = 100 kN/mm; D_f = 0.02), operating at rated speed (n_N = 2990 r/min)

shows that mainly the natural frequencies of the 4th mode and the 5th mode are influenced by the magnetic spring constant. The natural frequencies of the other modes are hardly influenced by the magnetic spring constant. The reason is that for the 4th mode and the 5th mode the relative orbits between the rotor mass and the stator mass are large, compared to the other orbits. Large orbits of the rotor mass and of the stator mass occur for these two modes and both masses – the rotor mass and the stator mass – vibrate out of phase to each other (Fig. 11), which lead to large relative orbits between these two masses. Therefore, the electromagnetic interaction between these two masses is high and therefore a significant influence of the magnetic spring constant on the natural vibrations occurs for these two modes. In the 1st and 2nd mode the motor is acting like a one-mass system (Fig. 11) and nearly no relative movements between rotor mass and stator mass occur. Therefore the electromagnetic coupling between rotor and stator has nearly no influence on the natural frequencies of the first two modes. The 3th mode is mainly dominated by large relative orbits between the shaft journals and the bearing housings – compared to the other orbits – leading to high modal damping. A relative movement between the rotor mass and the stator occurs, but is not sufficient enough for a clear influence of the electromagnetic coupling. The 6th mode is mainly dominated by large orbits of the motor feet, compared to the other orbits. Again the relative movement of the stator and rotor is not sufficient enough that the electromagnetic coupling influences the natural frequency of this mode clearly. The modal damping values of all modes are only marginally influenced by the magnetic spring constant, only a small influence on the modal damping of the 4th mode is obvious.

4.5.4 Stiffness variation map regarding the foundation stiffness

The foundation stiffness values c_{fz} and c_{yz} are changed by multiplying the rated stiffness values $c_{fz,rated}$ and $c_{fy,rated}$ from Table 1 with a factor, called foundation stiffness factor k_{cf}.

$$\text{Vertical foundation stiffness:} \quad c_{fz} = k_{cf} \cdot c_{fz,rated} \tag{51}$$

$$\text{Horizontal foundation stiffness:} \quad c_{fy} = k_{cf} \cdot c_{fy,rated} \tag{52}$$

Therefore the vertical foundation stiffness c_{fz} and the horizontal foundation stiffness c_{fy} are here changed in equal measure by the foundation stiffness factor k_{cf}. The influence of the foundation stiffness at rated speed on the natural frequencies and on the modal damping is shown in Fig. 14.

It is shown that for a separation margin of 15% between the natural frequencies and the rotary frequency $\Omega/2\pi$ the foundation stiffness factor k_{cf} has to be in a range of 2.5…3.0. If the foundation stiffness factor is smaller than 2.5 the natural frequency of the 5th mode gets into the separation margin. If the foundation stiffness factor is bigger than 3.0 the natural frequency of the 4th mode gets into the separation margin. Both modes – 4th mode and 5th mode – have a modal damping less than 10% in the whole range of the considered foundation stiffness factor (k_{cf} = 0.5…4). Because of the low modal damping values of these two modes, the operation close to the natural frequencies of these both modes suppose to be critical. Therefore the first arbitrarily chosen foundation stiffness values ($c_{fz,rated}$ = 133 kN/mm; $c_{fy,rated}$ = 100 kN/mm) have to be increased by a factor of k_{cf} = 2.5…3.0. With the increased foundation stiffness values the foundation can still be indicated as a soft foundation, because the natural frequencies of the 1st mode and the 2nd mode – the mode

shapes are still the same as in Fig. 11 – are still low, lying in a range between 24 Hz and 26 Hz for the 1st mode and between 33 Hz and 35 Hz for the 2nd mode.

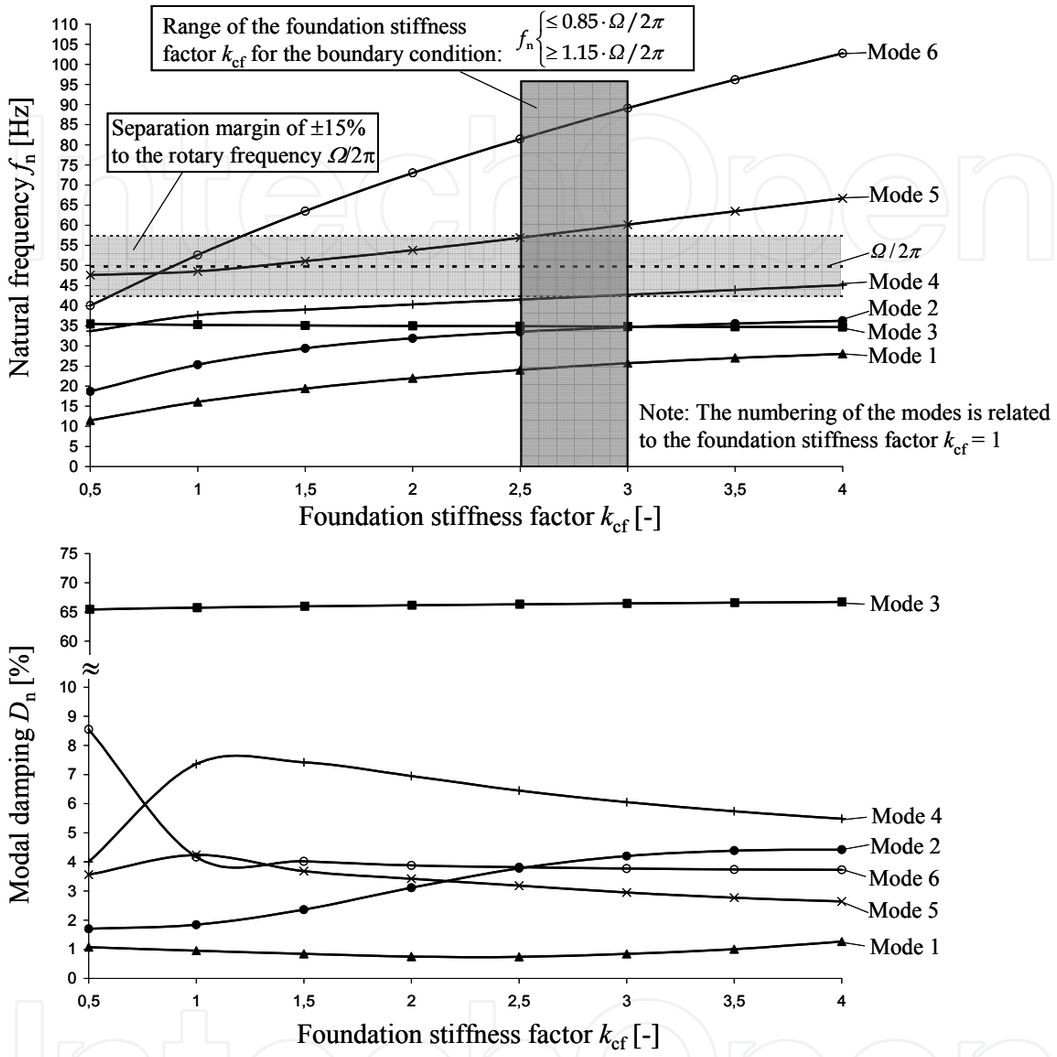

Fig. 14. Stiffness variation map regarding the foundation stiffness, motor mounted on a soft steel frame foundation, operating at rated speed (n_N = 2990 r/min)

5. Conclusion

The aim of this paper is to show a simplified plane vibration model, describing the natural vibrations in the transversal plane of soft mounted electrical machines, with flexible shafts and sleeve bearings. Based on the vibration model, the mathematical correlations between the rotor dynamics and the stator movement, the sleeve bearings, the electromagnetic and the foundation, are derived. For visualization, the natural vibrations of a soft mounted 2-pole induction motor are analyzed exemplary, for a rigid foundation and for a soft steel frame foundation. Additionally the influence of the electromagnetic interaction between rotor and stator on the natural vibrations is analyzed. Finally, the aim is not to replace a

detailed three-dimensional finite-element calculation by a simplified plane multibody model, but to show the mathematical correlations based on a simplified model.

6. References

Arkkio, A.; Antila, M.; Pokki, K.; Simon, A., Lantto, E. (2000). Electromagnetic force on a whirling cage rotor. *Proceedings of Electr. Power Appl.*, pp. 353-360, Vol. 147, No. 5

Belmans, R.; Vandenput, A.; Geysen, W. (1987). Calculation of the flux density and the unbalanced magnetic pull in two pole induction machines, pp. 151-161, *Arch. Elektrotech,* Volume 70

Bonello, P.; Brennan, M.J. (2001). Modelling the dynamic behaviour of a supercritcial rotor on a flexible foundation using the mechanical impedance technique, pp. 445-466, *Journal of sound and vibration*, Volume 239, Issue 3

Gasch, R.; Nordmann, R. ; Pfützner, H. (2002). *Rotordynamik,* Springer-Verlag, ISBN 3-540-41240-9, Berlin-Heidelberg

Gasch, R.; Maurer, J.; Sarfeld W. (1984). The influence of the elastic half space on stability and unbalance of a simple rotor-bearing foundation system, *Proceedings of Conference Vibration in Rotating Machinery,* pp. 1-11, C300/84, IMechE, Edinburgh

Glienicke, J. (1966). *Feder- und Dämpfungskonstanten von Gleitlagern für Turbomaschinen und deren Einfluss auf das Schwingungsverhalten eines einfachen Rotors*, Dissertation, Technische Hochschule Karlsruhe, Germany

Holopainen, T. P. (2004) *Electromechanical interaction in rotor dynamics of cage induction motors*, VTT Technical Research Centre of Finland, Ph.D. Thesis, Helsinki University of Technology, Finland

Kellenberger, W. (1987) *Elastisches Wuchten*, Springer-Verlag, ISBN 978-3540171232, Berlin-Heidelberg

Lund, J.; Thomsen, K. (1987). Review of the Concept of Dynamic Coefficients for Fluid Film Journal Bearings, pp. 37-41, *Journal of Tribology, Trans. ASME,* Vol. 109, No. 1

Lund, J.; Thomsen, K. (1978). A calculation method and data for the dynamics of oil lubricated journal bearings in fluid film bearings and rotor bearings system design and optimization, pp. 1-28, *Proceedings of Conference ASME Design and Engineering Conference,* ASME , New York

Schuisky, W. (1972). Magnetic pull in electrical machines due to the eccentricity of the rotor, pp. 391-399, *Electr. Res. Assoc. Trans*. 295

Seinsch, H-O. (1992). *Oberfelderscheinungen in Drehfeldmaschinen*, Teubner-Verlag, ISBN 3-519-06137-6, Stuttgart

Tondl, A. (1965). *Some problems of rotor dynamics*, Chapman & Hall, London

Vance, J.M.; Zeidan, F. J.; Murphy B. (2010). *Machinery Vibration and Rotordynamics*, John Wiley and Sons, ISBN 978-0-471-46213-2, Inc. Hoboken, New Jersey

Werner, U. (2010). Theoretical vibration analysis of soft mounted electrical machines regarding rotor eccentricity based on a multibody model, pp. 43-66, Springer, *Multibody System Dynamics*, Volume 24, No. 1, Berlin/Heidelberg

Werner, U. (2008). A mathematical model for lateral rotor dynamic analysis of soft mounted asynchronous machines. *ZAMM-Journal of Applied Mathematics and Mechanics*, pp. 910-924, Volume 88, No. 11

Werner, U. (2006). *Rotordynamische Analyse von Asynchronmaschinen mit magnetischen Unsymmetrien*, Dissertation, Technical University of Darmstadt, Germany, Shaker-Verlag, ISBN 3-8322-5330-0, Aachen

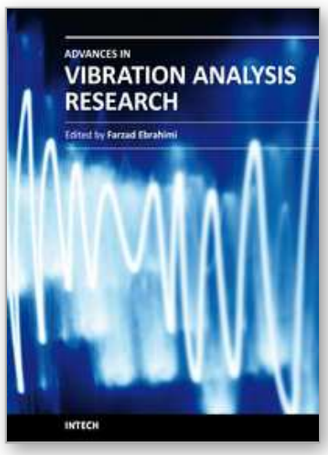

Advances in Vibration Analysis Research
Edited by Dr. Farzad Ebrahimi

ISBN 978-953-307-209-8
Hard cover, 456 pages
Publisher InTech
Published online 04, April, 2011
Published in print edition April, 2011

Vibrations are extremely important in all areas of human activities, for all sciences, technologies and industrial applications. Sometimes these Vibrations are useful but other times they are undesirable. In any case, understanding and analysis of vibrations are crucial. This book reports on the state of the art research and development findings on this very broad matter through 22 original and innovative research studies exhibiting various investigation directions. The present book is a result of contributions of experts from international scientific community working in different aspects of vibration analysis. The text is addressed not only to researchers, but also to professional engineers, students and other experts in a variety of disciplines, both academic and industrial seeking to gain a better understanding of what has been done in the field recently, and what kind of open problems are in this area.

InTech Europe
University Campus STeP Ri
Slavka Krautzeka 83/A
51000 Rijeka, Croatia
Phone: +385 (51) 770 447
Fax: +385 (51) 686 166
www.intechopen.com

InTech China
Unit 405, Office Block, Hotel Equatorial Shanghai
No.65, Yan An Road (West), Shanghai, 200040, China
中国上海市延安西路65号上海国际贵都大饭店办公楼405单元
Phone: +86-21-62489820
Fax: +86-21-62489821

IntechOpen